

Landing Rate Measurements to Detect Fibrinogen Adsorption to Non-fouling Surfaces

ASHUTOSH AGARWAL,¹ ELIZABETH LURIA,² XIAOPEI DENG,³ JOERG LAHANN,³ and HENRY HESS¹

¹Department of Biomedical Engineering, Columbia University, 351L Engineering Terrace MC 8904, 1210 Amsterdam Avenue, New York, NY 10027, USA; ²Department of Materials Science and Engineering, University of Florida, Gainesville, FL 32611, USA; and ³Department of Chemical Engineering, Department of Materials Engineering, and Macromolecular Science and Engineering Program, University of Michigan, Ann Arbor, MI 48109, USA

(Received 27 March 2012; accepted 26 June 2012; published online 10 July 2012)

Associate Editor David Sept oversaw the review of this article.

Abstract—Rapid advances in non-fouling surface technology have pushed the performance of novel coatings toward the detection limit of established protein density quantification techniques. Hence, there is an urgent need for more sensitive detection strategies. Previously we demonstrated that landing rate measurements of microtubules can reveal kinesin surface coverages between 0.1 and 10 μm^{-2} . In this report, we quantify the binding kinetics of highly fluorescent markers to surface-adsorbed proteins and demonstrate the use of protein surface densities in the range of 0.1–1000 μm^{-2} . We utilize this technique to measure kinesin densities on casein-coated glass surfaces and fibrinogen densities on non-fouling polyethylene glycol methacrylate (PEGMA) surfaces. The use of nanospheres (i) potentially permits the detection of a variety of adsorbed proteins, (ii) facilitates the determination of the landing rate due to their uniformity, and (iii) extends the dynamic range of the method due to their small size.

Keywords—Biomaterials, Coatings, Fibrinogen, Protein adsorption.

INTRODUCTION

The importance of protein resistant or ‘non-fouling’ coatings has been widely recognized,¹⁸ and has led to rapid advances in non-fouling surface coating technology.^{10,13,19,21,31} As a result of improved performance, quantitative evaluation of novel coatings is becoming increasingly challenging. While uncoated surfaces typically adsorb a monolayer of proteins (e.g., 350 ng cm^{-2} albumin and 600 ng cm^{-2} fibrinogen on a silicon surface),³⁰ non-fouling coatings can reduce adsorption to below 10 ng cm^{-2} ^{6,22,24} which already

represents the detection limit of many established protein density characterization techniques such as Ellipsometry,¹⁴ and Quartz Crystal Microbalance measurements.²⁷ The most sensitive commercially available biosensors are based on the Surface Plasmon Resonance technology and specialized systems achieve a detection limit of 0.1 ng cm^{-2} .¹⁵ Since blood protein coverages of $\sim 2 \text{ ng cm}^{-2}$ are sufficient to mediate platelet adhesion and subsequent clotting events,²³ it is critical to accurately measure protein density at these and lower levels to effectively differentiate between the performance of novel coating designs. In addition to the qualification of coatings for specific applications such as antibody arrays, or the design of anti-thrombogenic surfaces, accurate measurements of residual protein adsorption can also provide mechanistic insights into protein adsorption by providing dosage-density data over a wide range of protein dosages.

Landing rate measurements of fluorescent microtubule filament markers enable the determination of absolute coverages of adsorbed kinesin proteins in the range of 0.004–1 ng cm^{-2} .^{16,22} While this technique demonstrated outstanding sensitivity, it would be desirable to directly quantify the residual adsorption of the proteins of interest, such as blood proteins, rather than to rely on kinesin as a model indicator for general coating performance. The challenge is therefore to translate the landing rate methodology which affords single molecule sensitivity to a generic protein/marker combination.

Here, we demonstrate that measuring the landing rates of biotinylated fluorescent polystyrene nanospheres (40 nm diameter) can determine residual protein densities for both kinesin and fibrinogen. The biotinylated polystyrene nanospheres used in this study are chosen after screening biotinylated, carboxylated, sulfate-coated and amine coated nanospheres of

Address correspondence to Henry Hess, Department of Biomedical Engineering, Columbia University, 351L Engineering Terrace MC 8904, 1210 Amsterdam Avenue, New York, NY 10027, USA. Electronic mail: hh2374@columbia.edu

various sizes (40 nm, 200 nm and 1 μm) as well as fluorescent silica nanoparticles of various sizes. These nanospheres were selected because of their low rates of binding to surfaces without proteins and good binding rates to protein coated surfaces. We apply this technique first by measuring well-known kinesin densities on casein coated glass surfaces, and second by detecting fibrinogen densities on non-fouling polyethylene glycol methacrylate (PEGMA) coated surfaces.⁸

MATERIALS AND METHODS

Kinesin Adsorption to Casein Coated Glass

A kinesin construct consisting of the wild-type, full-length *Drosophila melanogaster* kinesin heavy chain and a C-terminal His-tag was expressed in *Escherichia coli* and purified using a Ni-NTA column.⁹ The assays were performed in 75 μm high and 1 cm wide flow cells assembled from two coverslips (Fisherfinest, Premium Cover Glass, #1, Fisher Scientific, Pittsburg, PA) and double-stick tape. The flow cell height was measured with a Dektak 6 M stylus profilometer (Veeco Instruments Inc.). Solutions were exchanged within a few seconds by pipetting the new solution to one side of the cell and removing the old solution using filter paper from the other side. First, a solution of casein (0.5 mg mL⁻¹, Sigma) dissolved in BRB80 (80 mM PIPES, 1 mM MgCl₂, 1 mM EGTA, pH 6.9) was injected into the flow cell. After 5 min, it was exchanged with a kinesin solution (varying dilutions from a stock concentration of ~14 μM in BRB80 with 0.5 mg mL⁻¹ casein and 1 mM AMPNP from Sigma). After 5 min, kinesin solution was washed out and biotin labeled polystyrene nanospheres loaded with fluorescein dye (40 nm FluoSpheres F8766, Invitrogen) at 100 pM concentration (diluted 5000 times in BRB80) were introduced into the flow cell and the time was recorded. Kinesin solution concentrations are measured by microtubule landing rate experiments and the known dilution factor (details in supporting information). It has been experimentally validated¹⁶ that for the herein studied range of kinesin concentrations, all kinesin in the solution adsorbs to the casein-coated glass surface resulting in total solution depletion. As a result, the kinesin surface density ρ can be determined from the initial kinesin concentration in solution c using $\rho = ch/2$ where h is the height of the flow cell.

PEGMA Coatings

Silicon (SVM Inc.) and glass coverslips (Thomas Scientific) were initially coated with approximately 50 nm poly[(*p*-xylylene-4-methyl-2-bromoisobutyrate)-

co-(*p*-xylylene)] *via* CVD polymerization. 80 mg [2.2]paracyclophane-4-methyl 2-bromoisobutyrate was sublimated at 90-100 °C and 0.3 mbar, went through thermal pyrolysis at 550 °C and then deposited at 15 °C on the substrate as a thin polymer film. Subsequently, PEGMA polymer brushes were coated *via* ATRP process onto the substrates as previously reported.²² The ATRP process was carried out overnight at room temperature. The coating thickness was around 200 nm as determined by ellipsometry (BASE-160 spectroscopic ellipsometer, J. A. Woollam, Inc.). Ellipsometric parameters were fitted using a Cauchy model.

Fibrinogen Adsorption to PEGMA Coated Glass

Fibrinogen (Human Fibrinogen Plasminogen, von Willebrand Factor and Fibronectin depleted, Enzyme Research Laboratories, South Bend, IN) was reconstituted in BRB80 buffer to obtain a stock concentration of 75 μM . The stock concentration was measured with UV spectrophotometry (NanoDrop 2000, Thermo Scientific). In all flow cells, the bottom surface and top cover surface had identical surface chemistry. First, BRB80 was flowed in and allowed to stand for 20 min. It was exchanged with varying fibrinogen dilutions in BRB80. After allowing 20 min for protein adsorption, the fibrinogen solution was washed out and nanospheres at 500 pM concentration (stock diluted 1000 times in BRB80) were introduced into the flow cell and the time was recorded.

Microscopy

Upon nanosphere injection, flow cells were mounted on the microscope stage and the time elapsed since nanosphere introduction was recorded using a digital stopwatch with one second accuracy. An 80 μm \times 80 μm area on the bottom surface of flow cells was imaged by epi-fluorescence microscopy using an Eclipse TE2000-U fluorescence microscope (Nikon, Melville, NY) with a 100 \times oil objective (N.A. 1.45), an X-cite 120 lamp (EXFO, Ontario, Canada), a FITC filter cube (#48001, Chroma Technologies, Rockingham, VT) and an iXon EMCCD camera (ANDOR, South Windsor, CT). Images were collected every 20 s with an exposure time of 0.2 s.

Determination of Attachment Rates and Surface Density

Nanosphere landing events were manually counted within a field-of-view using UTHSCSA ImageTool version 3.0 and plotted against time elapsed since nanosphere solution injection for each protein

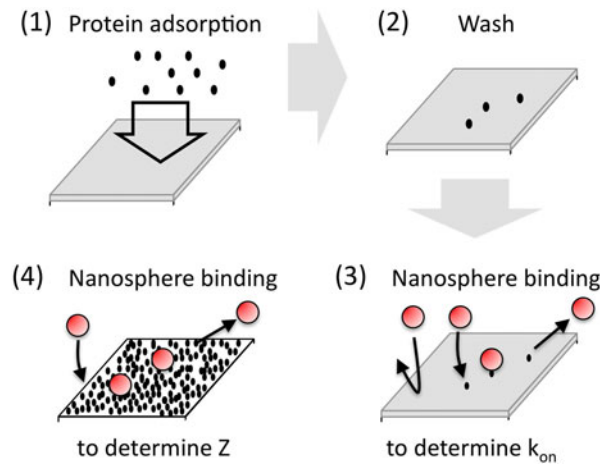


FIGURE 1. Sketch of principle. (1) The non-fouling coating is exposed to a protein solution. (2) After washing, a few proteins remain adsorbed. (3) A nanosphere solution is introduced. Most nanospheres do not encounter a protein when colliding with the surface. Some nanospheres encounter a protein and bind to it with a certain probability. Bound nanospheres are detected by fluorescence microscopy before they unbind again within minutes. (4) A protein-covered surface without a non-fouling coating is used to determine the maximal attachment rate.

dilution. Events are counted from the same field-of-view on a singular test surface for each protein dosage, and since the field-of-view is sampled at random and represents a small fraction of the test surface area, it is assumed that the counts follow a Poisson distribution. The number of counted events is an estimate of the mean of the distribution and also of its variance. The corresponding standard deviation is chosen as an estimate of the measurement error. The $N(t)$ plots were fitted (error weighted least squares) with Eq. (1) where N is the number of landed nanospheres (in a field-of-view of 0.0064 mm^2), t is the elapsed time, k_{on} is the attachment rate constant specific to that protein density and k_{off} is the detachment rate constant specific to that protein–nanosphere combination. The errors in the attachment and detachment rate constants represent the standard error in the fit parameters as determined by the fitting software (Origin, OriginLab Corp.) from the covariance matrix. Additionally, for PEGMA surfaces non-specific adsorption of nanospheres to bare PEGMA surfaces was observed. Hence, nanosphere landing events were recorded on bare PEGMA surfaces and the nanosphere landing events on PEGMA test surfaces were fitted by Eq. (1) after subtracting from each $N(t)$ value the corresponding number of nanospheres landed at the same time point on bare PEGMA surface (details in supporting information). The diffusion limited maximal landing rate, Z was assumed to be equal to the attachment rate observed on a bare glass surface for determining kinesin densities on casein-coated glass surface and equal to the attachment rate observed on fibrinogen monolayer for determining fibrinogen densities on PEGMA surface. Z was measured using the

same batch of diluted nanospheres to eliminate pipetting errors. A measurement of a finite k_{on}/Z (significantly different from zero) is the basis for the detection of surface adsorbed proteins at that protein concentration.

RESULTS AND DISCUSSION

Nanosphere Landing Rate Model for Protein Detection

The experimental procedure for nanosphere landing assays was similar to the methodology adopted for measuring microtubule landing rates²² and is illustrated in Fig. 1. After exposing test surfaces to protein solutions of known concentration, nanosphere solution was flowed in and time elapsed was recorded. The number of observed nanospheres, N , was manually counted and plotted against time elapsed since nanosphere injection, t , for each protein concentration. These data were fitted with a model which assumes that nanosphere landing events are reversible, that attachment is a zero order reaction (because of the large excess of protein binding sites on the surface and the negligible decline in solution concentration of nanospheres), and that detachment is a first order reaction (rate proportional to nanospheres landed on the surface). The data set for each experiment was fitted by the equation

$$N(t) = \frac{k_{\text{on}}}{k_{\text{off}}} [1 - \exp(-k_{\text{off}}t)] \quad (1)$$

where k_{on} and k_{off} are the attachment and detachment rate constants, respectively. Since the detachment of a

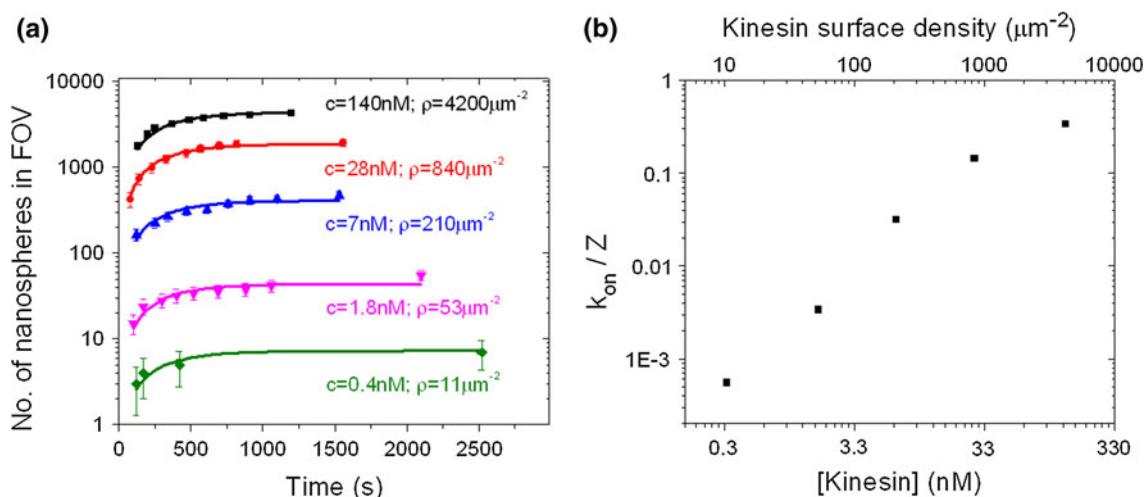


FIGURE 2. Measurement of kinesin surface densities on casein-coated glass from landing rates of nanospheres. (a) Number of nanospheres attached to the surface as a function of time for the casein-coated glass exposed to a series of kinesin dilutions from the stock solution within a field-of-view of $80 \mu\text{m} \times 80 \mu\text{m}$. The kinesin stock concentration was $1.4 \mu\text{M}$ and surfaces were exposed to kinesin for 5 min. Error bars represent standard deviation. (b) Relative attachment rate constants computed by dividing attachment rate constants with the diffusion limited maximal landing rate determined on a bare glass surface. The error bars are roughly the size of the data points and represent the standard error.

bound nanosphere occurs from a protein site, an identical detachment rate constant k_{off} was used in the fits for all protein concentrations. Since attachment occurs *via* collisions between solution suspended nanospheres and protein sites, k_{on} can be expressed as a product of the maximal, diffusion-limited attachment rate Z and the sticking probability of each collision.

The maximal attachment rate constant Z can be experimentally determined by fitting Eq. (1) to landing events measured on a highly adsorbing surface using the same dilution of nanosphere solution. Furthermore, if we assume the relative attachment rate constant (k_{on}/Z) to be equal to the probability of a colliding nanosphere to find at least one of the randomly distributed protein molecules on the surface, it can be related to the protein surface density, ρ according to

$$k_{\text{on}}/Z = [1 - \exp(-\rho A)] \quad (2)$$

where A is the surface area within which an incoming nanosphere and the surface bound protein interact. This area of interaction can be determined by measuring the relative attachment rate constant (k_{on}/Z) for known protein densities. Finally, unknown protein surface densities can be quantified using A , Z and the attachment rate constant k_{on} , according to $\rho = -[\ln(1 - k_{\text{on}}/Z)]/A$.

Detection of Kinesin on Casein Coated Glass

Kinesin adsorption on casein-coated glass surfaces is well understood^{3,26} and quantified.²² The

replacement of the fluorescent microtubule markers, which have a broad size distribution,²⁰ with commercially available biotinylated fluorescent nanospheres of uniform size (40 nm diameter) as markers was motivated by the observation that these nanospheres do not attach to casein-coated glass unless kinesin is present on the surface.^{4,11} Furthermore, nanosphere landing events were quantified for each kinesin concentration and are plotted in Fig. 2a. The data are fit to Eq. (1) to determine an attachment rate constant, k_{on} for each concentration. The detachment rate constant k_{off} was required to be the same for all concentrations, and the fit determined a value of $0.0036 \pm 0.0003 \text{ s}^{-1}$ (Mean \pm SD, $N = 5$). The maximal attachment rate constant Z was experimentally determined to be equal to $7210 \pm 10 \text{ s}^{-1} \text{ mm}^{-2}$ by fitting Eq. (1) to landing events measured on a highly adsorbing bare glass surface using the same nanosphere solution. Relative attachment rate constants, (k_{on}/Z), are shown in Fig. 2b.

Kinesin solution concentration and dosage dependent kinesin densities on casein-coated glass were determined using microtubule landing rate experiments (details in supporting information). Densities were determined in the range of $10 \mu\text{m}^{-2}$ to $4200 \mu\text{m}^{-2}$ and, by fitting the first four datapoints in Fig. 2b to Eq. (2), the nanosphere-kinesin area of interaction, A was estimated as $180 \pm 20 \text{ nm}^2$. The last datapoint deviates from the expected proportionality of the landing rate to the solution concentration due to crowding of kinesin (kinesin motor domains tethered by a 50 nm long flexible tail with a radius of gyration of 10 nm) on the surface at densities exceeding $1500 \mu\text{m}^{-2}$.

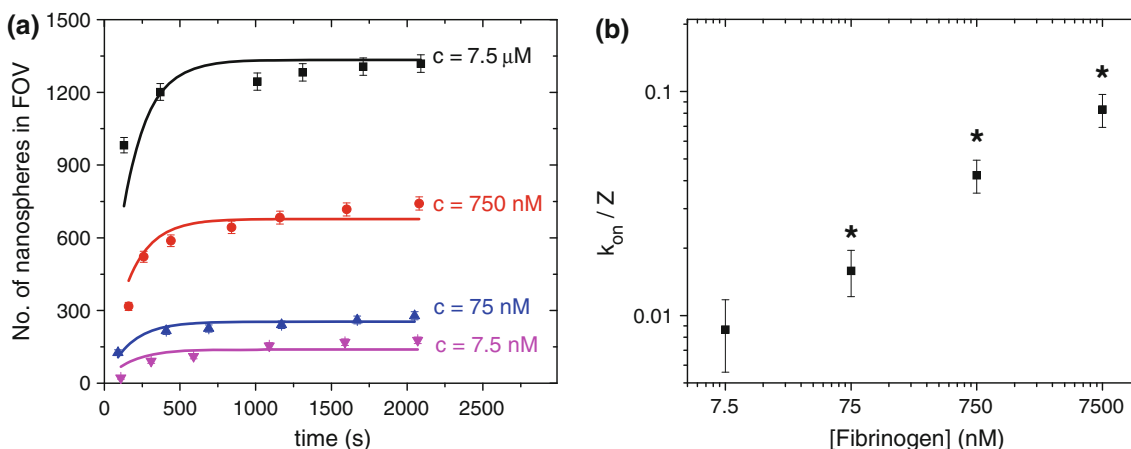


FIGURE 3. Measurement of fibrinogen surface densities on PEGMA from landing rates of nanospheres. (a) Number of nanospheres attached to the surface as a function of time for the PEGMA surfaces exposed to a series of fibrinogen dilutions from the stock solution in a field-of-view of $80\ \mu\text{m} \times 80\ \mu\text{m}$. Fibrinogen stock concentration was $75\ \mu\text{M}$ and surfaces were exposed to fibrinogen for 20 min. Error bars represent the standard deviation. (b) The relative attachment rate constants are computed by dividing attachment rate constants with the diffusion limited maximal landing rate determined on a fibrinogen monolayer and are approximately equal to the product of fibrinogen surface density and the fibrinogen–nanosphere interaction area. Error bars represent the standard error and * indicates statistical difference from zero ($p < 0.05$).

The use of nanospheres instead of microtubules shifts the dynamic range of the detection technique due to the changing interaction area. Microtubules with an average length of $4\ \mu\text{m}$ have a typical interaction area of $100,000\ \text{nm}^2$ while the nanosphere-protein area was determined to be less than $1000\ \text{nm}^2$. The measurements are sensitive while (k_{on}/Z) is still in the ‘linear regime’ and that occurs when (ρA) is less than unity. Therefore the upper detection limit increases to $1000\ \mu\text{m}^{-2}$. The lower detection limit is given by the need to observe a few bound nanospheres in a field of view, which in our conditions translates into $10\ \mu\text{m}^{-2}$. However, the sensitivity can be readily increased by increasing the concentration of nanospheres in the solution.

Detection of Fibrinogen on PEGMA Coated Glass

After establishing the feasibility of using nanospheres rather than microtubules as markers of protein adsorption, we aimed to quantify the adsorption of blood proteins, specifically fibrinogen, instead of kinesin onto non-fouling surfaces, specifically PEGMA-coated surfaces. Fibrinogen is an important blood protein in biomaterial surface design studies because of its critical role in hemostasis and thrombosis.^{12,25} Past evaluation of PEGMA surfaces has established that their non-fouling performance is exceptionally high.²² Flow cells were first assembled from PEGMA coated glass surfaces and exposed to fibrinogen dilutions of $7.5\ \mu\text{M}$ to $7.5\ \text{nM}$. A concentration of $7.5\ \mu\text{M}$ roughly represents the fibrinogen levels in blood⁵ and a concentration of $0.75\ \mu\text{M}$ is sufficient to form a monolayer on glass.^{1,7} Hence the range of fibrinogen dosages

represented the concentration of fibrinogen in blood to the concentration required to attain 1% monolayer coverage on a fouling surface.

The fit of all datasets to Eq. (1) (Fig. 3a) revealed a k_{off} of $0.0061 \pm 0.0009\ \text{s}^{-1}$ (Mean \pm SD, $N = 5$). The two detachment rate constants are significantly different from each other ($p = 0.03$). The maximal landing rate Z was determined by fitting Eq. (1) to nanosphere landing rates on a fibrinogen monolayer created on a glass surface by non-specific adsorption of fibrinogen. The corresponding relative attachment rate constants, (k_{on}/Z) , for each dilution are plotted in Fig. 3b.

Figure 3b shows that if fibrinogen is used as a probe for a PEGMA surface, the relative attachment rate constants do not increase linearly, but rather with the third root of the fibrinogen concentration in the solution. We believe that this slow increase in the attachment rate constant reflects a slow increase in the fibrinogen surface density, rather than negative cooperativity in the attachment of nanospheres to the fibrinogen for three reasons: (1) The nanospheres are well separated and evenly distributed across the surface while the low landing rate implies a low surface coverage of fibrinogen, which makes it unlikely that fibrinogen absorbs in dense islands where each nanosphere bound by one fibrinogen obscures additional fibrinogens. (2) Hucknall *et al.*¹⁷ observed similar absorption kinetics of OPG and IL-6 antigens to antibodies buried in poly(oligo(ethylene glycol) methacrylate) brush coatings (POEGMA coatings) of 100 nm thickness. This implies that the antigens showed the same behavior in finding the immobilized antibodies as the fibrinogen molecules in finding open

binding sites. (3) Since adsorption of proteins into defect sites of a non-fouling coating is similar to adsorption in porous media, a Freundlich isotherm ($\theta = KC^b$) could be expected to describe the adsorption process.²⁸

Ellipsometry measurements of fibrinogen adsorption (7.5 μM for 20 min) to PEGMA-coated silicon surfaces show that the fibrinogen adsorption even at the highest fibrinogen concentration used in this study is below the detection limit for ellipsometry. The average fibrinogen film thickness in three independent measurements was 0.12 nm with a standard deviation of 0.21 nm. The fibrinogen film thickness on surfaces without PEGMA coating (PPX-N surfaces, see methods) was 5.2 ± 0.25 nm which we assume corresponds to a monolayer, and since a monolayer of fibrinogen has a coverage of 8400 molecules μm^{-2} the implied fibrinogen–nanosphere interaction area is 400 ± 700 nm².

As a result of the large uncertainty in the fibrinogen–nanosphere interaction area, an absolute calibration of the fibrinogen surface density is not feasible with the current data. While experiments on surfaces which allow the simultaneous measurement of fibrinogen surface density with the landing rate method and a reference method are in principle possible, and would provide an exact number for the fibrinogen–nanosphere interaction area, knowledge of the absolute protein surface density is often of secondary interest. Instead, the focus is frequently on the relative performance of two coatings and is quantified by the brightness stemming from the adsorption of fluorescently labeled proteins²⁹ or the resonance frequency shift in a Surface Plasmon Resonance measurement.²⁴ As has been previously shown for landing rate measurements with kinesin proteins as probes and microtubules as markers,²² landing rate measurements can deliver this information, and now with an extended dynamic range due to the smaller interaction area of the nanosphere markers.

We recognize that a detailed understanding of the origins of these desirable interactions is still missing and the use of the same adsorption model for nanosphere binding to two different proteins is an approximation. Some deviation of the data from our Langmuir-type adsorption model can be seen in Fig. 3a (and Fig. S1), and can be expected for nanosphere binding to proteins adsorbed with varying accessibility in the 200 nm thick polymeric coatings. The utilization of a more complex adsorption model is left to future studies.

In conclusion, we have demonstrated that certain fluorescent nanospheres can be used in landing rate measurements as non-specific markers for protein adsorption to non-fouling surfaces. Their small size relative to the previously used microtubule markers

increases the dynamic range of the landing rate method by two orders of magnitude while maintaining the lower detection limit of only 0.1 protein molecules μm^{-2} (~ 0.005 ng cm⁻²). The nonspecific nature of the protein–nanosphere interaction enables the detection not only of kinesin, but also of proteins with relevance to coagulation and thrombosis, such as fibrinogen.

ELECTRONIC SUPPLEMENTARY MATERIAL

The online version of this article (doi: [10.1007/s12195-012-0239-6](https://doi.org/10.1007/s12195-012-0239-6)) contains supplementary material, which is available to authorized users.

ACKNOWLEDGMENTS

The authors thank Amit Singh of PERC, University of Florida, and Siheng He for helpful discussions. H.H. was supported by NSF Award DMR 1015486.

CONFLICT OF INTEREST

The authors do not have any conflict of interest to declare.

REFERENCES

- Adamczyk, Z., J. Barbasz, and M. Ciesla. Kinetics of fibrinogen adsorption on hydrophilic substrates. *Langmuir* 27:6868–6878, 2011.
- Adamczyk, Z., P. Belouschek, and D. Lorenz. Electrostatic interactions of bodies bearing thin double-layers, I. General formulation. *Ber. Bunsenges. Phys. Chem.* 94:1483–1492, 1990.
- Agarwal, A., and H. Hess. Biomolecular motors at the intersection of nanotechnology and polymer science. *Prog. Polym. Sci.* 35:252–277, 2010.
- Agarwal, A., P. Katira, and H. Hess. Millisecond curing time of a molecular adhesive causes velocity-dependent cargo-loading of molecular shuttles. *Nano. Lett.* 9:1170–1175, 2009.
- Black, J. *Biological Performance of Materials* (4th ed.). Boca Raton: Taylor & Francis, 2006.
- Cao, L., M. Chang, C.-Y. Lee, D. G. Castner, S. Sukavaneshvar, B. D. Ratner, and T. A. Horbett. Plasma-deposited tetraglyme surfaces greatly reduce total blood protein adsorption, contact activation, platelet adhesion, platelet procoagulant activity, and *in vitro* thrombus deposition. *J. Biomed. Mater. Res. A* 81A:827–837, 2007.
- Chan, B. M. C., and J. L. Brash. Adsorption of fibrinogen on glass: reversibility aspects. *J. Colloid. Interf. Sci.* 82:217–225, 1981.
- Chen, H. Y., and J. Lahann. Fabrication of discontinuous surface patterns within microfluidic channels using photodefinable vapor-based polymer coatings. *Anal. Chem.* 77:6909–6914, 2005.
- Coy, D. L., M. Wagenbach, and J. Howard. Kinesin takes one 8-nm step for each ATP that it hydrolyzes. *J. Biol. Chem.* 274:3667–3671, 1999.

- ¹⁰Estephan, Z. G., J. B. Schlenoff, and P. S. Schlenoff. Zwitteration as an alternative to PEGylation. *Langmuir* 27:6794–6800, 2011.
- ¹¹Fischer, T., A. Agarwal, and H. Hess. A smart dust biosensor powered by kinesin motors. *Nat. Nanotechnol.* 4:162–166, 2009.
- ¹²Gombotz, W. R., W. Guanghui, T. A. Horbett, and A. S. Hoffman. Protein adsorption to poly(ethylene oxide) surfaces. *J. Biomed. Mater. Res.* 25:1547–1562, 1991.
- ¹³Gon, S., M. Bendersky, J. L. Ross, and M. M. Santore. Manipulating protein adsorption using a patchy protein-resistant brush. *Langmuir* 26:12147–12154, 2010.
- ¹⁴Hansson, K. M., S. Tosatti, J. Isaksson, J. Wettero, M. Textor, T. L. Lindahl, and P. Tengvall. Whole blood coagulation on protein adsorption-resistant PEG and peptide functionalised PEG-coated titanium surfaces. *Biomaterials* 26:861–872, 2005.
- ¹⁵Hoa, X. D., A. G. Kirk, and M. Tabrizian. Towards integrated and sensitive surface plasmon resonance biosensors: a review of recent progress. *Biosens. Bioelectron.* 23:151–160, 2007.
- ¹⁶Howard, J., A. J. Hudspeth, and R. D. Vale. Movement of microtubules by single kinesin molecules. *Nature* 342:154–158, 1989.
- ¹⁷Hucknall, A., D.-H. Kim, S. Rangarajan, R. T. Hill, W. M. Reichert, and A. Chilkoti. Simple fabrication of antibody microarrays on nonfouling polymer brushes with femtomolar sensitivity for protein analytes in serum and blood. *Adv. Mater.* 21:1968–1971, 2009.
- ¹⁸Hucknall, A., S. Rangarajan, and A. Chilkoti. In pursuit of zero: polymer brushes that resist the adsorption of proteins. *Adv. Mater.* 21:2441–2446, 2009.
- ¹⁹Ionov, L., A. Synytska, E. Kaul, and S. Diez. Protein-resistant polymer coatings based on surface-adsorbed poly (aminoethyl methacrylate)/poly (ethylene glycol) copolymers. *Biomacromolecules* 11:233–237, 2010.
- ²⁰Jeune-Smith, Y., and H. Hess. Engineering the length distribution of microtubules polymerized *in vitro*. *Soft Matter* 6:1778–1784, 2010.
- ²¹Jiang, S. Y., and Z. Q. Cao. Ultralow-fouling, functionalizable, and hydrolyzable zwitterionic materials and their derivatives for biological applications. *Adv. Mater.* 22:920–932, 2010.
- ²²Katira, P., A. Agarwal, T. Fischer, H.-Y. Chen, X. Jiang, J. Lahann, and H. Hess. Quantifying the performance of protein-resisting surfaces at ultra-low protein coverages using kinesin motor proteins as probes. *Adv. Mater.* 19:3171–3176, 2007.
- ²³Kwak, D., Y. G. Wu, and T. A. Horbett. Fibrinogen and von Willebrand's factor adsorption are both required for platelet adhesion from sheared suspensions to polyethylene preadsorbed with blood plasma. *J. Biomed. Mater. Res. A* 74A:69–83, 2005.
- ²⁴Ma, H., J. Hyun, P. Stiller, and A. Chilkoti. “Non-fouling” oligo (ethylene glycol)-functionalized polymer brushes synthesized by surface-initiated atom transfer radical polymerization. *Adv. Mater.* 16:338–341, 2004.
- ²⁵Mosesson, M. W. Fibrin polymerization and its regulatory role in hemostasis. *J. Lab. Clin. Med.* 116:8–17, 1990.
- ²⁶Ozeki, T., V. Verma, M. Uppalapati, Y. Suzuki, M. Nakamura, J. M. Catchmark, and W. O. Hancock. Surface-bound casein modulates the adsorption and activity of kinesin on SiO₂ surfaces. *Biophys. J.* 96:3305–3318, 2009.
- ²⁷Rodriguez-Pardo, L., J. F. Rodriguez, C. Gabrielli, and R. Brendel. Sensitivity, noise, and resolution in QCM sensors in liquid media. *IEEE Sens. J.* 5:1251–1257, 2005.
- ²⁸Skopp, J. Derivation of the Freundlich Adsorption Isotherm from Kinetics. *J. Chem. Educ.* 86:1341–1343, 2009.
- ²⁹Suh, K. Y., R. Langer, and J. Lahann. A novel photodefinable reactive polymer coating and its use for microfabrication of hydrogel elements. *Adv. Mater.* 16:1401–1405, 2004.
- ³⁰Zhang, M. Q., T. Desai, and M. Ferrari. Proteins and cells on PEG immobilized silicon surfaces. *Biomaterials* 19:953–960, 1998.
- ³¹Zhang, Z., M. Zhang, S. F. Chen, T. A. Horbetta, B. D. Ratner, and S. Y. Jiang. Blood compatibility of surfaces with superlow protein adsorption. *Biomaterials* 29:4285–4291, 2008.